International Journal of Automotive Technology, Vol. 6, No. 5, pp. 483–489 (2005)

1229–9138/2005/023–07

STUDY ON RIDE QUALITY OF A HEAVY-DUTY OFF-ROAD VEHICLE WITH A NONLINEAR HYDROPNEUMATIC SPRING

T. SUN* and F. YU

School of Mechanical Engineering, Institute for Automotive Engineering,
Shanghai Jiaotong University, Shanghai 200030, China

(Received 4 June 2004; Revised 19 April 2005)

ABSTRACT–Based on a two-degree of freedom vehicle model, this paper investigates ride comfort for a heavy off-road vehicle mounted a nonlinear hydropneumatic spring, which is influenced by nonlinear stiffness and damping characteristics of the hydropneumatic spring. Especially, the damping force is derived by applying H. Blasius formula in modeling process according to the real physical structure of the hydropneumatic spring, and the established model of nonlinear stiffness characteristics have been validated by experiments. Furthermore, the effects of parameter variations of the hydropneumatic spring, such as initial charge pressure and damping coefficient, on body acceleration, suspension deflection and dynamic tire deflection are also investigated.

KEY WORDS : Hydropneumatic spring, Nonlinear characteristics, Ride comfort, Heavy off-road vehicle

NOMENCLATURE

A	: sectional area of restriction orifice, (m^2)
A_1	: area of main piston, (m^2)
A_2	: area of floating piston, (m^2)
a	: ratio of area between main piston and floating piston
C_d	: flow coefficient related with restriction orifices in compression or rebound stroke
C_{reb}	: damping coefficient of rebound, ($Ns^{1.75}/m^{1.75}$)
C_{com}	: damping coefficient of compression, ($Ns^{1.75}/m^{1.75}$)
C_n	: damping coefficient, ($Ns^{1.75}/m^{1.75}$)
D	: diameter of restriction orifice, (m)
d	: diameter of fluid flow cross-section, (m)
F	: operating load, (N)
f_0	: Lower Cut-off frequency, (Hz)
G_0	: coefficient of road roughness, (m^2/m^{-1})
H_0	: static equilibrium reduced height of accumulator, (m)
h	: floating piston displacement, (m)
K_t	: stiffness of tire, (kN/m)
K_s	: stiffness of suspension, (kN/m)
L	: length of restriction channel, (m)
m_s	: sprung mass, (kg)
m_{us}	: unsprung mass, (kg)
p_g	: instant gas pressure of accumulator, (pa)
p_0	: static equilibrium pressure of accumulator, (pa)
p_1	: oil pressure of oil cylinder, (pa)
p_2	: oil pressure in accumulator, (pa)
Q	: volume flow rate, (m^3/s)
R_e	: Reynolds number
r	: polytropic exponent
v_0	: vehicle velocity, (m/s)
V_t	: instant volume of accumulator, (m^3)
V_0	: static equilibrium gas volume of accumulator, (m^3)
V_{oil1}	: volume of oil in I chamber, (m^3)
V_{oil2}	: volume of oil in¢Úchamber, (m^3)
w	: white noise input with mean = 0 and variance = 1
x	: piston rod displacement, (m)
$\dot{x}$	: piston rod velocity, (m/s)
z_s	: vertical displacement of sprung mass, (m)
z_u	: vertical displacement of unsprung mass, (m)
z_r	: vertical displacement of road input, (m)
Δp	: pressure drop in restriction orifice, (pa)
ν	: kinematic viscosity of oil, (m^2/s)
$\bar{\nu}$	: fluid flow velocity, (m/s)
ρ	: density of oil, (kg/m^3)
β_e	: the volume modulus of operating oil, (N/m^2)

**Corresponding author.* e-mail: tao_sun@sjtu.edu.cn

1. INTRODUCTION

With increasing of vehicle speed in ground transportation, more attention has been paid to the arising health problems of operators of heavy off-road vehicles in recent years. In particular, emphasis has been put on the improvement of ride comfort, which is more contribution to the vibration isolation of operators. High-mobility vehicles, such as military tanks and armored personnel carriers, are designed for mobility over rough off-road terrain surfaces in order to improve the ability of rapid response. The mobility performance of these vehicles is often limited by the operator's endurance to withstand the transmitted shocks and vibrations, and his ability to maintain control. The maximum allowable vehicle speed (or ride limiting speed) varies with the roughness of a particular terrain, and is primarily influenced by the suspension system design (Maclaurin, 1983; Hoogterp *et al.*, 1993). Heavy off-road vehicles with conventional suspension which is generally consisted of shock absorber and coil springs, are difficult to accommodate the rough off-road at relative high speed, however, the present trend is to use the hydropneumatic spring to attenuate the shock and vibration caused by road irregularities. It is known that considerable improvements to heavy off-road vehicles' speed and passenger comfort could be made by use of hydropneumatic spring due to their nonlinear progressively stiffening spring characteristics. By employing a hydropneumatic spring, the objectives of increasing vehicle speed, alleviating shock and reducing bumps can be achieved, so they are widely used in military vehicles and various heavy ones.

Aiming at a heavy off-road vehicle with hydropneumatic suspensions, this paper firstly analyzes nonlinear characteristics of hydropneumatic suspension by setting up its mathematical model of nonlinear gas spring force and damping force. Especially, the damping force is derived by applying H. Blasius (Sullivan, 1989; Koenraad *et al.*, 1994) formula considering the real structure of the damping metallic plate in modeling process rather than that assumption the damping force is conventionally proportional to relative velocity. Secondly, by introduction the nonlinear characteristics of hydropneumatic spring into vehicle model, ride quality is simulated and evaluated. Finally, ride quality including body acceleration, suspension deflection and dynamic tire deflection is investigated considering parameter variations of hydropneumatic suspension, such as initial charge pressure and damping coefficient.

2. HYDROPNEUMATIC SPRING MODELING

Hydropneumatic suspension system is generally composed of hydropneumatic spring and guide mechanism, in which ride quality of the heavy off-road vehicle is mainly affected by the properties of the hydropneumatic spring, as schematically shown in Figure 1 – Figure 3, which consists of a mono-accumulator with an oil-gas separated floating piston and a shock absorber in structure. When the piston rod moves upwards and oil is compressed, pressure p_1 of chamber I increases and the restriction

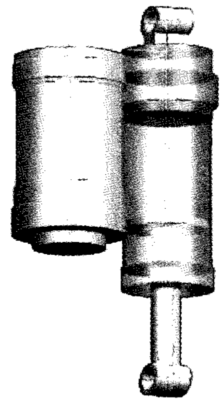

Figure 1. Solid model of a hydropneumatic spring.

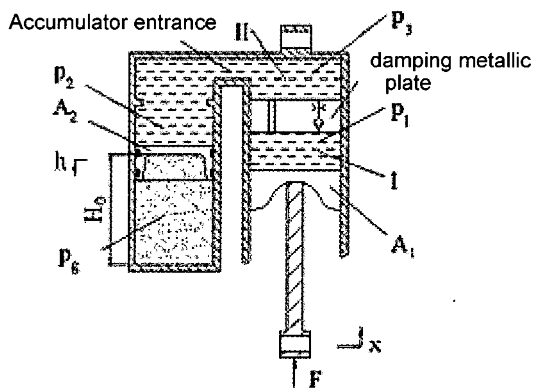

Figure 2. Schematic diagram of a hydropneumatic spring.

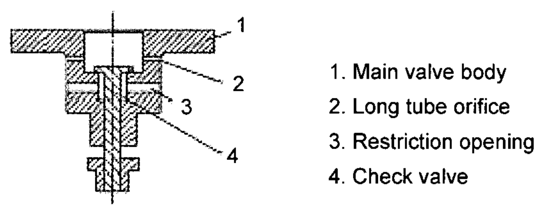

Figure 3. Schematic diagram of a damping metallic plate.

orifice is open at preset pressure value, then oil passes through it into a pressure accumulator which results in augmentation in pressure of p_2, simultaneously the floating piston moves downwards, as hydropneumatic spring is in the state of compressed stroke. As the piston rod is pulled out of the oil cylinder body (rebound stroke), covering physical process is reverse.

2.1. Nonlinear Stiffening Spring Characteristics

The total force of hydropneumatic spring consists of damping force, gas-spring force and friction force. The friction force is generally negligible in modeling considering of lubrication condition as the hydropneumatic spring working.

In view of practical structure of a hydropneumatic spring for the heavy off-road vehicle, the mathematical model of stiffness is derived as following:

The equations of static equilibrium position of a piston rod is expressed as:

$$F = p_1 A_1 \tag{1}$$

$$p_1 = p_2 = p_g \tag{2}$$

The displacement between piston rod and floating piston could be given by:

$$A_1 x = A_2 h \tag{3}$$

The thermodynamic state equation of accumulator could be expressed as:

$$p_g V_t^r = p_0 V_0^r \tag{4}$$

$$p_g (H_0 - h)^r = p_0 H_0^r \tag{5}$$

Solving Equations (1) – (5), simultaneously, by letting $A_1/A_2 = a$, the gas-spring force could be derived as the following form:

$$F_{gas-spring} = \frac{A_1 p_0}{(1 - ax/H_0)^r} \tag{6}$$

The hydropneumatic spring has a remarkable characteristic that is nonlinear progressively stiffening spring characteristics. Different stiffness characteristic curves can be obtained by varying initial charge pressure to adapt vehicles with different weight. The stiffness property of the hydropneumatic spring has been experimentally validated, as shown in Figure 4, where the dotted line and circle represents experimental data, and the solid line represents the simulation results. In a certain range, simulation results have shown the similarity to the experimental data, however, deviation happens beyond 150mm in suspension stroke. It results from two aspects. One is that polytropic exponent make large with temperature rising due to adiabatic compression. The other is as a result of conversion from friction to thermo energy, which we have neglected in modeling. From stiffness coefficient versus time curve, in Figure 5, it can be seen that stiffness characteristic is mainly concerned to compression stroke of the hydropneumatic spring, and is not obvious in rebound stroke for the single acting hydropneumatic spring. Additionally, with initial charge pressure raised, the hydropneumatic spring stiffness becomes small.

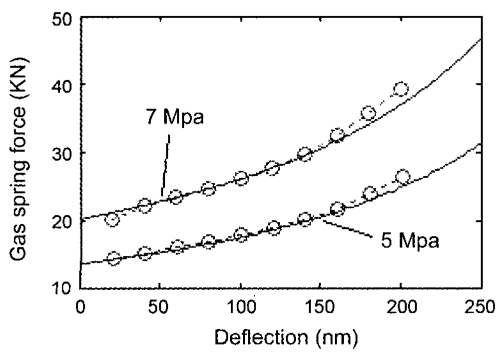

Figure 4. Gas spring force-deflection diagram.

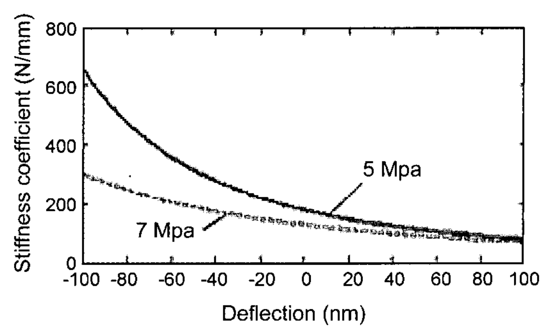

Figure 5. Stiffness coefficient-deflection diagram.

2.2. Nonlinear Damping Force Characteristics

The nonlinear damping force is modeled by applying H. Blasius formula according to the structure of damping metallic plate of the hydropneumatic spring. Obviously, it differs from the conventional approach, which is assumed that the damping force is proportional to relative velocity. In addition, oil compressibility and flow resistance in parallel and in series are also considered in modeling of nonlinear damping force.

$$\Delta p = \frac{0.3164}{R_e^{0.25}} \frac{L}{D} \cdot \frac{\rho Q^2}{2A^2} \tag{7}$$

$$Re = \frac{\bar{v} d}{\nu} \tag{8}$$

Solving Equations (7) and (8), simultaneously, so:

$$\Delta p = 0.1582 \frac{L}{D^{1.25} A^{1.75}} \rho \nu^{0.25} Q^{1.75} \tag{9}$$

The total pressure drop between small orifice in parallel and flow rate could be derived as:

$$\Delta P_{total} = 0.1582 \rho \nu^{0.25} Q^{1.75} \left[\sum_{i=1}^{n} \left(\frac{D_i^{1.25} A_i^{1.75}}{L_i} \right)^{\frac{1}{1.75}} \right]^{-1.75} sign(\dot{x}) \tag{10}$$

In addition, local pressure loss of long channel between accumulator and oil cylinder should be considered by applying H. Blasius formula, so the pressure drop may be expressed as the following form:

$$\Delta p_{32} = 0.1582 \frac{L_{tube}}{D_{tube}^{1.25} A_{tube}^{1.75}} \rho v^{0.25} Q^{1.75} sign(\dot{x}) \quad (11)$$

Here, the variables involved are L_{tube}, D_{tube}, A_{tube}, Δp_{32} which denotes length, diameter, cross sectional area and port pressure drop of long channel respectively. Considering flow rate variation caused by compressible fluid of oil, equations are derived as below:

$$Q = A_1 \dot{x} - Q_{comp} sign(\dot{x}) \quad (12)$$

Where

$$Q_{comp} = \frac{V_{oil2}}{\beta_e} \frac{dp_g}{dt} + \frac{V_{oil1}}{\beta_e} \frac{dp_1}{dt}$$

The nonlinear damping force of the hydropneumatic spring can be obtained by the Equation (13).

$$F_{damping} = C_{damping} \dot{x}^{1.75} = C_{damping} (Q/A_1)^{1.75}$$

$$C_{damping} = 0.1582 A_1^{2.75} \rho v^{0.25} C_d sign(\dot{x}) \quad (13)$$

The total force acting on piston rod of hydropneumatic spring can be given by Equation (14).

$$F_{damper} + F_{gas-sping} + F_{damping} = \frac{A_1 p_0}{(1 - ax/H_0)^r} - 0.1582 A_1 \rho v^{0.25} Q^{1.75} C_d sign(\dot{x}) \quad (14)$$

Simulation results of force and deflection loops excited by sinusoidal signal are presented in Figure 6 and force-relative velocity loops are shown in Figure 7, which are the results of combined action of damping force and gas-spring force of the hydropneumatic spring. From the analysis of simulation results, it is found that the shape of the curves shows remarkably asymmetric£¨which mainly results from the difference of force characteristics in different stroke of the hydropneumatic spring. It shows predomination of the gas-spring force as the hydropneumatic spring is compressible, on the contrary, damping characteristic is more remarkably in rebound stroke, and thus more vibration energy is dissipated. Moreover, with the frequency increases, magnitude of damping force becomes predominant at high excitation frequencies and thus yields the deterioration of vibration isolation effect.

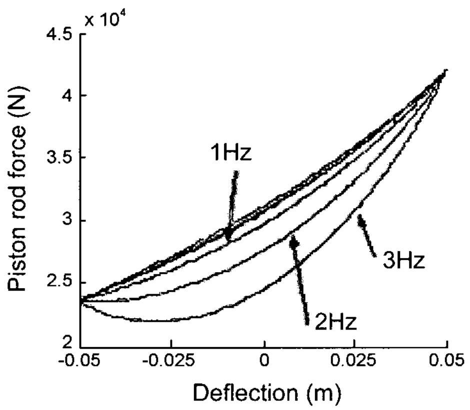

Figure 6. Load-deflection loops.

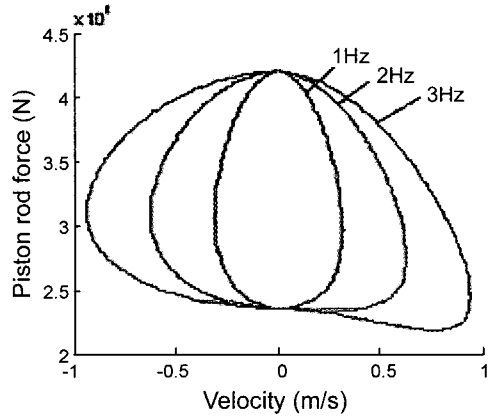

Figure 7. Load-velocity loops.

3. MODELING OF A VEHICLE SUSPENSION

A vehicle suspension, equipped with passive hydropneumatic spring, is modeled as a two-degree-of-freedom (2-Dof) dynamical system (Chalasani, 1986), and analyzed to evaluate the shock and vibration isolation performance, as shown in Figure 8.

The vehicle mass is represented by a sprung mass m_s, and wheel and axle assembly is modeled as an unsprung mass m_{us}. Primary vehicle suspension model comprises of a linearized spring with the stiffness K_s, and a passive hydraulic damper with a linearized damping coefficient C_s. The tire is modeled as a linear spring with stiffness K_t. The hysteretic properties of the tire are assumed to be

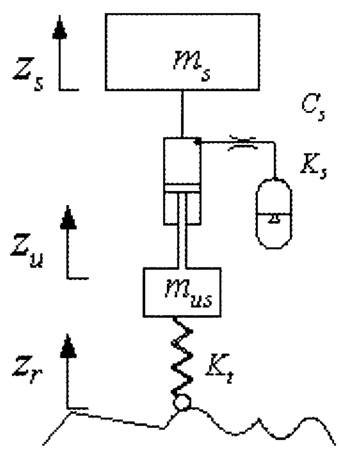

Figure 8. A quarter vehicle model.

small. Equations of the 2-Dof vehicle model can then be expressed as:

$$m_s\ddot{z}_s + C_s(\dot{z}_s - \dot{z}_u) + K_s(z_s - z_u) = 0 \tag{15}$$

$$m_{us}\ddot{z}_t + C_s(\dot{z}_u - \dot{z}_s) + K_s(z_u - z_s) + K_t(z_u - z_r) = 0 \tag{16}$$

But total force generated by the hydropneumatic spring including a nonlinear restoring force due to gas-spring and a nonlinear dissipative force due to restriction flows, which is given by formula (14) should substitute for linear damping force and linear spring force denoted by formula (15) and (16), so the detailed nonlinear differential equations of this 2-Dof vehicle model are obtained as follows:

$$m_s\ddot{z}_s + C_n\left|(\dot{z}_s - \dot{z}_u)\right|^{1.75} + m_s g - \frac{m_s g}{[1 - a(z_s - z_u)/H_0]^r} = 0 \tag{17}$$

$$m_{us}\ddot{z}_u - C_n\left|(\dot{z}_u - \dot{z}_s)\right|^{1.75} - m_s g + \frac{m_s g}{[1 - a(z_s - z_u)/H_0]^r} + K_t(z_u - z_r) = 0 \tag{18}$$

$$C_n = \left\{ C_{reb}\frac{[1 + sign(\dot{z}_s - \dot{z}_u)]}{2} + C_{com}\frac{[1 - sign(\dot{z}_s - \dot{z}_u)]}{2} \right\} \cdot sign(\dot{z}_s - \dot{z}_u)$$

In order to investigate ride quality of the heavy off-road vehicle, the road excitation of the wheel by a filtered white noise is described as (Yu *et al.*, 1998, 2000):

$$\dot{z}_r = -2\pi f_0 z_r + 2\pi\sqrt{G_o v_0 w} \tag{19}$$

4. SIMULATION AND RESULTS ANALYSIS

In this section, nonlinear characteristics are introduced to a 2-Dof vehicle model with the following simulation parameters. And then, the effects of variations of initial charge pressure and damping coefficients of the hydropneumatic spring on ride comfort have been analyzed in the following simulation.

Simulation parameters:

m_s = 3120 kg; m_{us} = 615 kg; K_t = 600 kN/m; A_1 = 0.003318 m^2; H_0 = 0.180 m (7 Mpa); a = 0.5216; C_{com} = 2533.4 Ns$^{1.75}$/m$^{1.75}$; C_{reb} = 6781.6 Ns$^{1.75}$/m$^{1.75}$; v_0 =45 km/h; f_0 =0.125 Hz; P_0 = 9.21 Mpa; ν = 20 mm^2/s; G_0 = 1024×10^{-6} m^2/m^{-1} (D type of road);

The selection of damping coefficient and stiffness of the hydropneumatic spring must guarantee the ride comfort quality of the heavy-duty vehicle on the rough road condition. Therefore, we select D type of road at the speed of 45 kilometer per hour to evaluate the dynamic response of vehicle ride performance. The vertical acceleration of wheel acceleration, body acceleration,

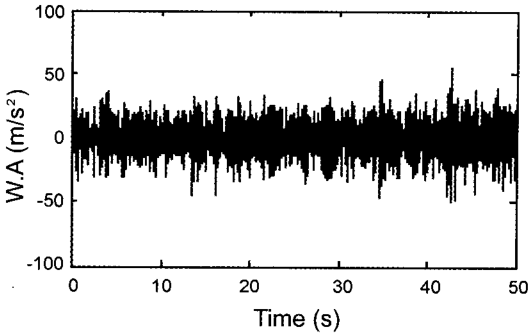

Figure 9. Acceleration response of unsprung mass.

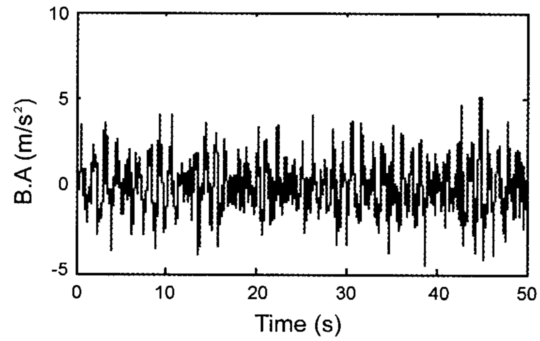

Figure 10. Acceleration response of sprung mass.

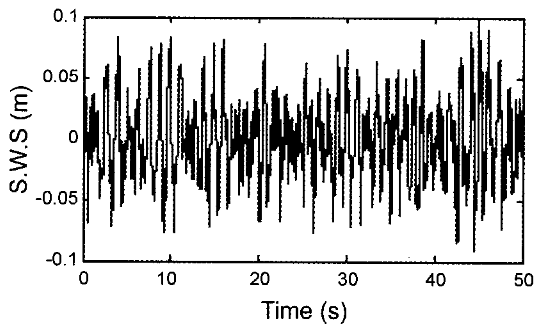

Figure 11. Suspension dynamic deflection.

suspension stroke and damper force are analyzed at the condition mentioned above, as shown in Figure 9 – Figure 12 respectively. It can be seen that the nonlinear hydropneumatic spring plays an important role on vibration suppression from the road irregularities. Magnitude of body acceleration is remarkably reduced, meanwhile, suspension stroke sustains in the range of the design value (± 100 mm).

There are two distinguishing features in the hydropneumatic spring. One is stiffness characteristic variation by changing the initial charge pressure of accumulator. The other is a trade-off between damping coefficient and

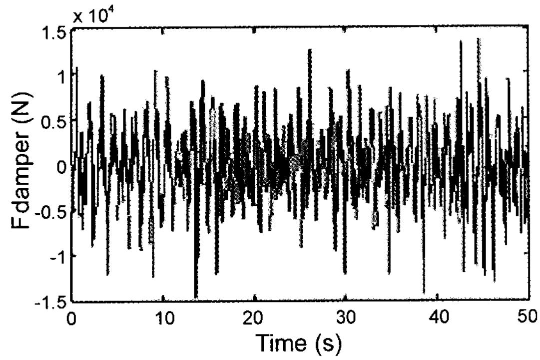

Figure 12. Resulted damper force.

Table 1. Comparisons of RMS of ride performance at initial charge pressure variations.

Ride performance	D type of road		
	7 pa	5 Mpa	3 Mpa
BA (m/s^2)	1.357	1.800	2.6727
SWS (mm)	31.36	30.91	29.51
DTD (mm)	13.39	14.01	16.54

spring stiffness in order to achieve maximum of ride comfort. It could be achieved greater stiffness by decreasing initial charge pressure of the hydropneumatic spring with its value of 7 Mpa, 5 Mpa, 3 Mpa, respectively, as shown in Table 1. It can be seen that smaller body acceleration has been obtained at initial charge pressure of 7 Mpa at the same damping setting. Magnitude of suspension stroke and dynamic tire deflection at other initial charge pressures is not far different from initial charge pressure of 7 Mpa. So initial charge pressure at 7 Mpa is more proper as D type of road condition as concerned.

Ride quality relates to not only stiffness characteristic, but also damping configuration of the hydropneumatic spring. Damping coefficient has been designed by different numerical value to investigate the effects of ride performance. Four groups of damping coefficients, which is once, twice, fourth and sixth as much as initial damping coefficient of C_{com} and C_{reb} respectively, and their roles on ride quality are shown as Table 2. From Table 2, some valuable results can be obtained. Group one, initial damping coefficient designed, is a little smaller than other configurations of damping coefficient considering root mean square (RMS) of body acceleration increased comparing the others, but full advantages of suspension stroke is taken when vehicle driven on D type of road. When damping coefficient is twice as much as initial damping coefficient, it can be obtained that a 10 percent decrease in RMS of body acceleration and a 17 percent decrease in RMS of dynamic tire deflection has been

Table 2. Comparisons of RMS of ride performance at damping coefficient variations.

Classification of damping coefficients	*BA* (m/s^2)	*SWS* (mm)	*DTD* (mm)
1	1.357	31.36	13.39
2	1.227	25.61	11.13
3	1.202	21.11	9.772
4	1.234	19.04	9.382

achieved. From simulation results of the fourth damping configuration, as damping coefficient reaches to a certain numerical value, RMS of body acceleration has increased reversely. These facts indicate that damping coefficient should be limited in a numerical range for the aim of improving ride quality of off-road vehicle. In that range, obviously, increasing damping coefficient is at the expense of decreasing the diameter of orifices or increasing the viscosity of oil, and the fewer diameters of restriction orifices makes, the more possible restriction orifice is obstructed. Additionally, softer suspension could play a more important role on absorption of shock considering the off-road vehicle ride conditions, so it is more beneficial for ride comfort and handling performance on rough terrains. In a sense, damping coefficient and stiffness of the hydropneumatic spring need to be considered in a compromise way for the aim of improving ride quality.

5. CONCLUSIONS

In this paper, nonlinear modeling is presented as an effective design approach for analyzing ride performance of a heavy off-road vehicle containing nonlinear characteristics variations of a hydropneumatic spring. By the analysis above, it is found that nonlinear properties of the hydropneumatic spring could effectively improve ride comfort of the heavy off-road vehicle on rough terrains. Moreover, parameters selection, such as initial charge pressure and damping coefficient should be considered as a trade-off between ride quality and reasonable suspension working space according to the simulation results. Finally, the analysis above provides design guideline for the semi-active or active hydropneumatic spring furthermore.

ACKNOWLEDGEMENT–The authors are grateful for supports from the Special Research Foundation of Ph.D. Study in University of China under Grant No. 20020248042.

REFERENCES

Chalasani, R. M. (1986). Ride performance potential of active suspension systems – Part I Simplified analysis on a quarter-car model. *Proc. Symposium on Simulation* *and Control of Ground Vehicles and Transportation Systems*, Anaheim, Cal, 187–204.

Hoogterp, F. B., Saxon, N. L. and Schihl, P. J. (1993). Semi-active suspensions for military vehicles. *SAE Paper No.* 930847.

Koenraad, Reybrouck, Monroe Europe (1994). A non linear parametric model of an automotive shock absorber. *SAE Paper No.* 940869.

Maclaurin, B. (1983). Progress in British tracked vehicle suspension systems. *SAE Paper No.* 830442.

Sullivan, J. A. (1989). *Fluid Power Theory and Applications.* 3rd edn. Prentice Hall. New Jersey.

Yu, F. and Crolla, D. A. (1998). Design of kalman active vhicle suspension system using wheelbase preview control. *Proc. Int.Conference on Advances in Vehicle Control and Safety*, Amiens, France, 453–459.

Yu, F., Zhang, J.-W. and Crolla, D. A. (2000). A study of a kalman filter active vehicle suspension system using correlation of front and rear wheel road inputs. *Int. J. Automobile Engineering*, **214,** 493–502.